Energy and Buildings 87 (2015) 176–184

Contents lists available at ScienceDirect

Energy and Buildings

journal homepage: www.elsevier.com/locate/enbuild

Fractional-order adaptive minimum energy cognitive lighting control strategy for the hybrid lighting system☆

Chun Yin[a,b,*], Brandon Stark[b], YangQuan Chen[b], Shou-ming Zhong[c], Erik Lau[b]

[a] School of Automation Engineering, University of Electronic Science and Technology of China, Chengdu 611731, PR China
[b] Mechatronics, Embedded Systems and Automation (MESA) Lab, School of Engineering, University of California, l Merced, 5200 North Lake Road, Merced, CA 95343, USA
[c] School of Mathematics Science, University of Electronic Science and Technology of China, Chengdu 611731, PR China

ARTICLE INFO

Article history:
Received 7 April 2014
Received in revised form 2 October 2014
Accepted 12 November 2014
Available online 20 November 2014

Keywords:
Fractional-order cognitive lighting control
Minimum electric energy usage
Hybrid lighting system
Fractional-order extremum seeking control
Proportional integral derivative controller
Stability region

ABSTRACT

In this paper, a fractional-order (FO) adaptive minimum energy cognitive lighting control strategy is developed to minimize the energy usage in a hybrid lighting system. A hardware-in-the-loop prototype of a cognitive hybrid lighting control plant is designed and built. The FO lighting control strategy is the combination between an FO extremum seeking controller (ESC) and a proportional integral derivative (PID) controller. The FO ESC guarantees the minimized energy usage, while the PID controller is applied to achieve a comfortable light level. The FO ESC demonstrates an improved convergence speed and accuracy. The experimental results are presented to demonstrate the practicality and effectiveness of the proposed FO minimum energy cognitive lighting control scheme.

1. Introduction

In today's society, electric lighting is a major energy consumer due to the significant demand of huge illumination. Therefore, one important requirement is huge electrical energy saving, which is possible by developing energy efficient devices, effective controls and design. One useful way to save electric energy consumption for lighting is to supplement artificial light with natural light, known as hybrid lighting [1–4]. In Refs. [5–11], lighting energy saving based on minimizing illuminance has been investigated by linear programming method. Hybrid lighting can be further optimized by finding the minimum energy necessary for the desired illumination levels by manipulating different light sources. In order to find a global solution, a concept of adaptive minimum energy cognitive lighting control has been proposed to maintain the desired light level and minimization of energy usage in our previous work [12,13].

The minimum energy usage changes with different environmental conditions, such as the natural illumination. Hence, this problem about minimum energy usage point tracking can be solved by extremum seeking control (ESC) law [14–16]. To obtain a better control performance, Yin et al. [13] have developed an FO sliding mode based ESC law to the hybrid lighting.

In this paper, a hardware-in-the-loop prototype of an adaptive minimum energy cognitive lighting control is proposed, designed and built. Combining the hardware Arduino Prototyping Platform [17] and the simulator for embedded systems, an Arduino-based miniature two story smart house is built as a physical test plant. First, it is shown that the two story house under the PID controller can help the house obtain the desired amount of light. Next, a nonlinear illumination-energy usage characteristic is measured and visualized. It can be utilized to analyzed how to minimize the electricity energy usage while keeping the desired light level.

An FO ESC with a PI^{1-q} switching surface is proposed as the part of the FO adaptive minimum energy cognitive lighting control strategy. It is utilized to guarantee that the energy consumption in the lighting system can reach within an arbitrary small vicinity of the minimum energy usage and stays on it thereafter. Furthermore, the flexibility in fractional order makes the FO ESC a more useful tool in obtaining a faster convergence speed and a higher control accuracy.

☆ This work was supported by National Basic Research Program of China (2010CB732501) and the Program for New Century Excellent Talents in University (NCET-10-0097).

* Corresponding author at: School of Automation Engineering, University of Electronic Science and Technology of China, Chengdu 611731, PR China.
Tel.: +86 13880488086.
E-mail addresses: yinchun.86416@163.com (C. Yin), brandon.stark@gmail.com (B. Stark), yqchen@ieee.org (Y. Chen), zhongsm@uestc.edu.cn (S.-m. Zhong).

http://dx.doi.org/10.1016/j.enbuild.2014.11.036
0378-7788/

The experimental results are presented to show the effectiveness of the proposed minimum energy cognitive lighting control scheme.

2. Lighting system description

2.1. Problem formulation

Hybrid lighting is a useful way to cut electric consumption in lighting system. Since natural light remains complex to operate, hybrid lighting must have active control of light levels at all times. Hence, an adaptive minimum energy cognitive lighting control strategy can be implemented to minimize the consumption, as shown in Fig. 1.

To minimize the electric energy usage, light sensors can provide the feedback to the hybrid lighting system. Then, the goal of maintaining the desired light level can be achieved by separately adjusting the brightness of individual lights, changing the electric energy usage. Hence, the FO ESC can be applied to find the energy needed for each light that minimizes the total energy consumption.

2.2. System description

In order to illustrate the situation, an Arduino-based miniature two story smart house is built as follows: The Arduino, a programmable prototyping platform with seemingly limitless capabilities of environment sensing and actuation, is used in the lighting system. A free add-on package, called ArduinoIO, allows the Arduino to act as a data acquisition board (DAQ) for MATLAB and Simulink. The architecture of the Arduino-based miniature house is depicted in Fig. 2.

The Arduino-based miniature house is 12″ height, 12″ length and 16″ width, as illustrated in Fig. 3. In every floor, it has 6 light-emitting diodes (LEDs) and a light sensor. In order to show how to achieve the minimum electric energy usage, we just use the first floor to make experiment. As illustrated in Fig. 4, the light sensor in this floor is in the middle of the table and the six LEDs are divided into two groups: (1) front lights (i.e. front three lights) that are near the window; (2) back lights (i.e. back three lights).

The aim of this paper is to minimize the electric energy usage of the Arduino based miniature house by automatically adjusting two groups, while bringing the indoor illumination to the desired light level. *There exist two loops: (a) the first loop is applied to maintain the desired light level; (b) the second loop is used to minimize energy usage in such the above condition.*

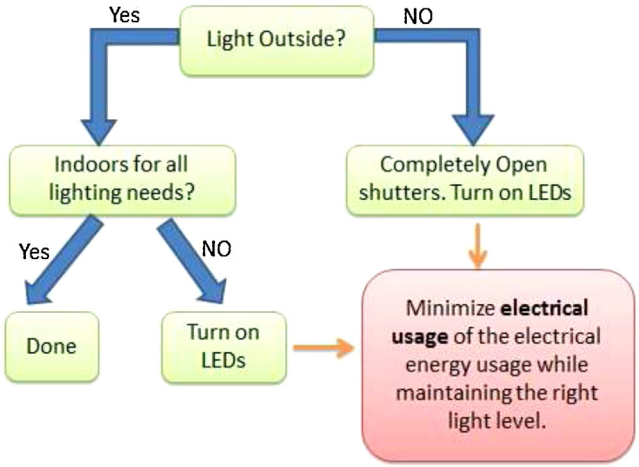

Fig. 1. Minimum energy cognitive lighting control strategy schematic.

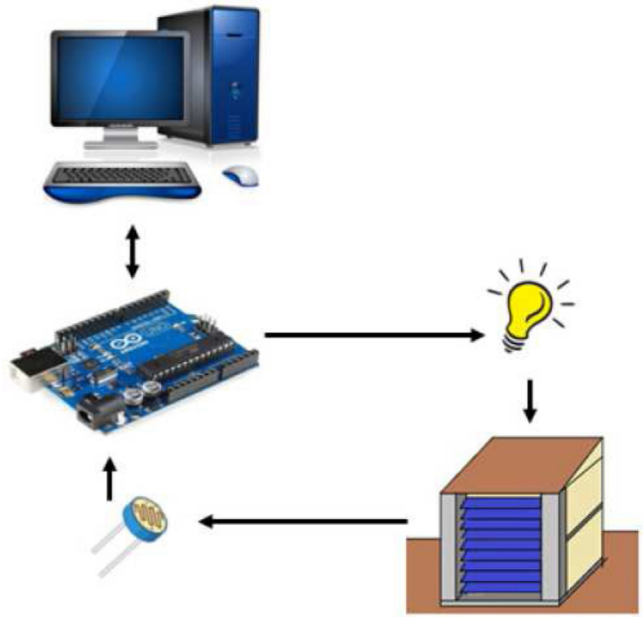

Fig. 2. The Arduino-based physical test plant developed at MESA Lab of UC Merced.

Fig. 3. Arduino-based miniature two story smart house.

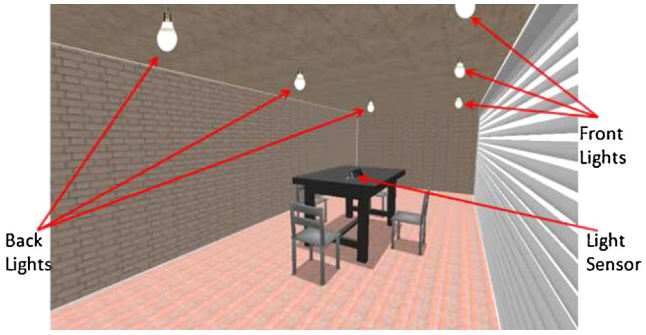

Fig. 4. The indoor of first floor in the Arduino-based two story smart house.

In the whole loop, I denotes the output of current source, to maintain the desired light level. I is split into two parts I_1 and I_2. I_1 indicates the current that is used in the front lights and I_2 denotes the current that is used in the back lights. The following equations describe the current ($I = I_1 + I_2$) and electric energy usage(E)

$$E = I_1^2 + I_2^2, \tag{1}$$

$$I_1 = \omega I, \quad I_2 = (1-\omega)I, \tag{2}$$

where the parameter ω satisfies $0 \le \omega \le 1$.

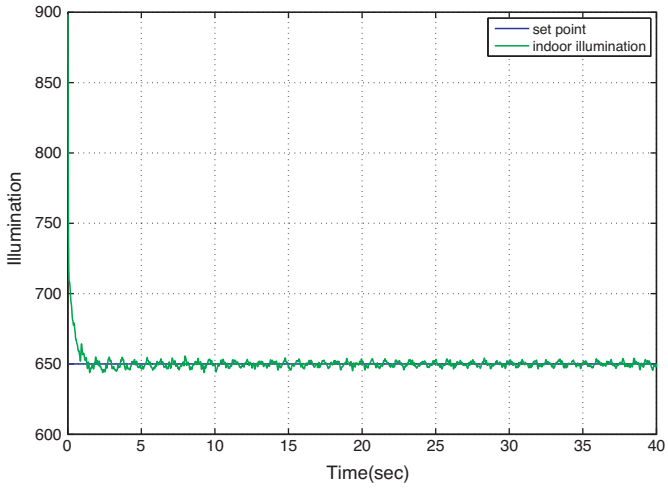

Fig. 5. The illumination of the Arduino-based smart house under PID control.

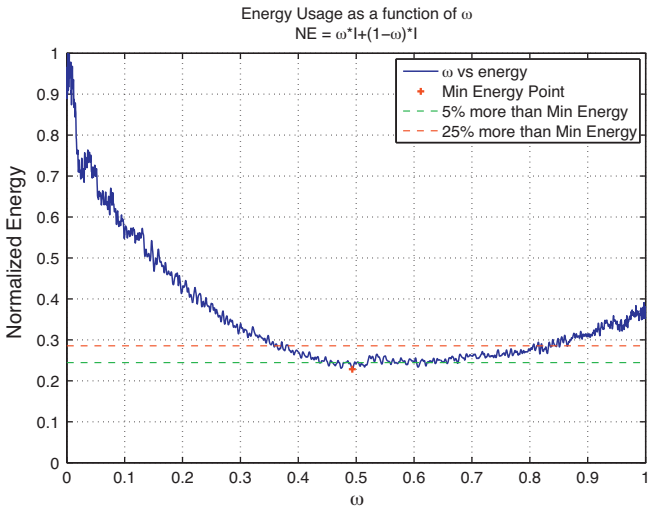

Fig. 6. E–ω curve, while the indoor illumination reaches the desired lighting level.

The objective is to drive the electric energy usage E to the minimum energy usage point E^* and remain on such point thereafter, as closely as possible.

To set up the experiment and validation, first it is shown that the inner loop PID controller can maintain a desired level of light. First, a constant natural light and a desired light level are assumed. The desired light level is set to an arbitrary level (see Appendix A), somewhere within the reachable level of light that the hardware can provide [18]. It is shown in Fig. 5, that the desired light level can be reached with the Arduino-based smart house.

To demonstrate that there exists a minimum energy usage at the desired light level, the change in E versus ω is depicted in Fig. 6. It is visible that there exists an optimal ω^* such that E arrives at E^*. Next, the ESC with the FO PI sliding surface will be introduced and implemented in the hardware-in-the-loop test bench to achieve the second loop. In this paper, the energy usage shown is normalized. In Fig. 6, the minimal energy usage is about 0.2283 at $\omega^* = 0.4933$ in the above situation.

3. Fractional-order extremum seeking control with sliding modes principle

3.1. Problem formulation

First, consider a single-input single-output (SISO) nonlinear system [15,16]

$$\frac{d}{dt}x = f(x,u), \quad y = \tilde{F}(x), \tag{3}$$

where $x \in R^n$, $u \in R$, $y \in R$ are the state, control input and output. The functions $f(x,u)$ and $\tilde{F}(x)$ are smooth. Though the goal is the minimization of y, it is assumed that there is no knowledge of $\tilde{F}(x)$. Consider the input control $u = \eta(x,\theta)$, is parameterized by a scalar parameter θ, such that $\frac{d}{dt}x = f(x,\eta(x,\theta))$.

Assumption 3.1. There exists a smooth function $x_e : R \to R^n$ such that $f(x,\eta(x,\theta)) = 0$ if and only if $x = x_e(\theta)$.

Assumption 3.2. At the equilibrium point $x_e(\theta)$, static performance map from θ to y, that is $y(t) = \tilde{F}(x_e(\theta)) = F(\theta)$, is smooth.

It is assumed that there exists a unique minimum point at θ^* for $F(\theta)$. Note that $dy/dt = F'(\theta)d\theta/dt$. By using $F'(\theta) = dF(\theta)/d\theta$, $F''(\theta) = d^2F(\theta)/d\theta^2$, the following assumption for the output function is listed.

Assumption 3.3. There exists a unique $\theta^* \in R$ such that $F'(\theta^*) = 0$ and $F''(\theta^*) > 0$. For any given $\varepsilon > 0$, there exists $\delta = \delta(\varepsilon)$ such that $|F'(\theta)| > \varepsilon$, $\forall \theta \notin D_\delta$, where $D_\delta = \{\theta : |\theta - \theta^*| < \delta/2\}$ is called δ-vicinity of θ^*.

In order to design the controller, the definition of fractional calculus and lemmas are recalled. The uniform formula of FO integral [19,20] is defined as follows ${}_0D_t^{-\alpha} f(t) = (1/\Gamma(\alpha)) \int_0^t (t-\tau)^{\alpha-1} f(\tau) d\tau$, where $\alpha > 0$, $f(t)$ is an arbitrary integrable function, $\Gamma(\cdot)$ is Gamma function. Furthermore, the Caputo FO derivative operator is given by ${}_0D_t^{\alpha} f(t) = (1/\Gamma(n-\alpha)) \int_0^t (t-\tau)^{n-\alpha-1} f^{(n)}(\tau) d\tau$, in which $n-1 < \alpha < n$.

Lemma 3.1. [21] *${}_0D_t^{\alpha} \varsigma = A\varsigma$, $\varsigma(0) = \varsigma_0$ is the autonomous system, where α is differential order, $\varsigma \in R^n$ and $A \in R^{n\times n}$, is asymptotically stable if $|\arg(eig(A))| > \alpha\pi/2$. In this case, each component of the states decays towards 0 like $t^{-\alpha}$. This system is stable if $|\arg(eig(A))| \geq \alpha\pi/2$ and those critical eigenvalues that satisfy $|\arg(eig(A))| = \alpha\pi/2$ have geometric multiplicity one.*

Lemma 3.2. [20] *The fractional integration operator ${}_aD_t^{-\beta}$ with fractional-order β, ($\beta \in C$, $\mathrm{Re}(\beta) > 0$), is bounded in $L_p(\tilde{a},\tilde{b})$, ($1 \leq p \leq \infty$, $-\infty < \tilde{a} < \tilde{b} < +\infty$):* $\|{}_aD_t^{-\beta} f\|_p \leq K \|f\|_p$, *($K = ((\tilde{b}-\tilde{a})^{\mathrm{Re}(\beta)})/(\mathrm{Re}(\beta)|\Gamma(\beta)|)$).*

3.2. Fractional-order sliding mode based extremum seeking control with PI^{1-q} sliding surface

FO controllers, such as ([13,22–24]) are important to the practical world. In this paper, an FO ESC with FO PI sliding surface will be designed for the system (1) (depicted in Fig. 7). First, θ is designed to satisfy $\dot{\theta} = v$, with v being variable structure control

$$v = \phi \mathrm{sgn}\left(\sin\left(\frac{\pi}{\gamma_0}\tau\right)\right), \tag{4}$$

where ϕ is a designed function, $\tau = \gamma_1 e + \gamma_2 ({}_0D_t^{q-1} e)$, $-1 < q \leq 0$, where $\gamma_i > 0$, ($i = 0, 1, 2$), q is fractional order. Define $e = y - y_r$, where $y_r(t) = -k_{r1}t^3 - k_{r2}t$, $y_r(0) = y_{r0}$, with $k_{r1} \geq 0$, $k_{r2} \geq 0$, and y_{r0} is the initial condition. In order to evade an unbounded signal, one can saturate y_r at a rough lower bound $\bar{B}$ of y^* without influencing the extremum search.

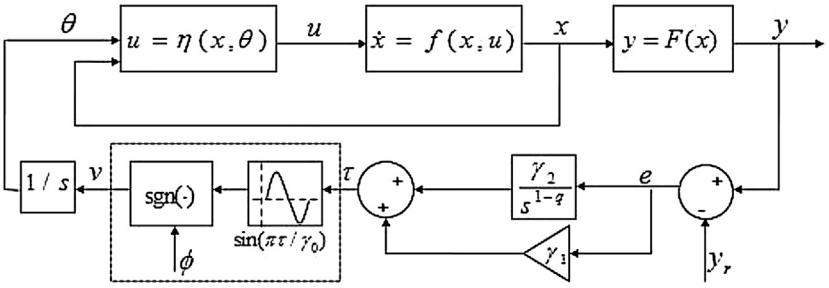

Fig. 7. Block diagram of fractional-order extremum seeking control with sliding modes system.

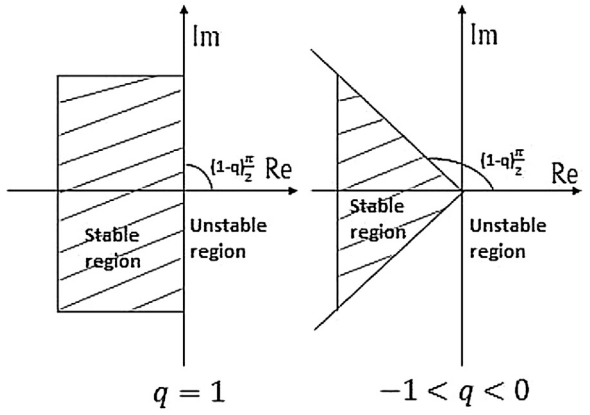

Fig. 8. Stability region of fractional system.

Remark 3.1. y^* may be constantly changing along with time. However, an lower bound for y^* exists which can be estimated. In order to have faster speed, y_{r0} could be selected such that y_{r0} is greater than the estimated lower bound.

Remark 3.2. ϕ will be deduced such that $\dot{\tau} = 0$ occurs in finite time on one of FO PI sliding manifolds $\tau = l\gamma_0$, with some integer l. One has ${}_0D_t^{1-q}e = -(\gamma_2/\gamma_1)e, \quad -1 < q \le 0$. From Lemma 3.1, the stable region for ${}_0D_t^{1-q}\varsigma = A\varsigma, \quad -1 < q \le 0$ is shown in Fig. 8. For ${}_0D_t^{1-q}e = -(\gamma_2/\gamma_1)e$, we have $|\arg(eig(A))| = \pi$ where $A = -\gamma_2/\gamma_1$. When $-1 < q \le 0$, $|\arg(eig(A))| > (1-q)\pi/2$ is constantly established. Hence, the dynamics is asymptotically stable. As a result, y is forced to y^* as long as y is away from a small vicinity of y^*.

4. Stability analysis of fractional-order extremum seeking control based on sliding modes

The stability analysis of the FO ESC with the PI^{1-q} sliding surface will be investigated. First, considering $-1 < q < 0$, the time derivative of $\tau(t)$ is obtained as

$$\dot{\tau}(t) = \gamma_1 F' v + \gamma_1 k_{r1} t^2 + \xi_s, \tag{5}$$

in which $\xi_s := \gamma_1 k_{r2} + \gamma_2({}_0D_t^q e)$. Denoting $k = \gamma_1 F'$, one has $\dot{\tau} = k(v + \vartheta)$, in which $\vartheta = \gamma_1 k_{r1} t^2/k + \varpi$ with $\varpi := (\gamma_1 k_{r2} + \gamma_2({}_0D_t^q e))/k$. Since $y \ge y_* > \overline{B}$ and $y_r > \overline{B}$, there exists $M > 0$ such that $|y - y_r| < M$. From Lemma 3.2, one has $|{}_0D_t^q e| < KM$. So, there exists $0 < \tilde{k} \le \gamma_1 \varepsilon$ such that $\tilde{k} \le |k|, \quad \forall \theta \notin D_\delta$. Hence, one has $|\varpi| \le \hat{\varpi}$ where $\hat{\varpi} = (\gamma_1 k_{r2} + \gamma_2 KM)/\tilde{k}$. Then, one possible ϕ will be given such that finite-time escape is avoided and realization of the FO sliding modes with $-1 < q < 0$ is guaranteed.

Theorem 4.1. *Consider the system (1–3) under FO ESC (4) with the PI^{1-q} sliding surface (8), where $-1 < q < 0$. Outside D_δ, if ϕ satisfies*

$$\phi := [(\gamma_1 k_{r2} + \gamma_2 KM)] + ||y_t|| e^{-\alpha_1 t}]/\tilde{k} + \alpha, \tag{6}$$

where $\alpha > 0, \alpha_1 > 0$, then, while $\theta \notin D_\delta$, one has (i): no finite-time escape happens in the system signals ($t_M \to +\infty$) and (ii) an FO PI sliding mode on $\tau(t) = l\gamma_0$ is realized in finite time for some integer l.

Proof. See Appendix B.

Next, it will be shown for $-1 < q < 0$ that FO ESC with the PI^{1-q} sliding surface guarantees that y can near around y^*, meanwhile θ remains or oscillates around D_δ.

Theorem 4.2. *Consider the system (1–3) under FO ESC (4) with the PI^{1-q} sliding surface (8) and the modulation function (6), in which $-1 < q < 0$. If Assumptions 3.1–3.3 hold, then: (i) D_δ is globally attractive and is achieved in finite time and (ii) for enough small γ_0, the oscillations around y^* of y can be made of order $O(\gamma_0)$.*

Proof. See Appendix C.

Next, consider $q = 0$, FO ESC (4) with the PI^{1-q} sliding surface (8) is the IO ESC with the PI sliding surface.

Remark 4.1. When $q = 0$, the time derivative of $\tau(t)$ is obtained as $\dot{\tau}(t) = \gamma_1 F' v + \gamma_1 k_{r1} t^2 + \xi_s$, in which $\xi_s := \gamma_1 k_{r2} + \gamma_2 e$. One has $\dot{\tau} = k(v + \vartheta)$ where $\vartheta := \gamma_1 k_{r1} t^2/k + \varpi$ with $\varpi = (\gamma_1 k_{r2} + \gamma_2 e)/k$. Similarly $-1 < q < 0$, one has $|\varpi| \le \tilde{\varpi}$, in which $\tilde{\varpi} \le (\gamma_1 k_{r2} + \gamma_2 M)/\tilde{k}$. Hence, one possible $\phi := [(\gamma_1 k_{r2} + \gamma_2 M)] + ||y_t|| e^{-\alpha_1 t}]/\tilde{k} + \alpha$ can ensure that y under the IO ESC can reach the vicinity of y^* and remain near it, thereafter. Due to space limit, the proof is not included, which is similar to the above proof.

5. Extension to multiple units case

In the real world, it should be considered that a few of identical units needs to be minimized. In one case, each of these units may own a different input concurrently, and the corresponding outputs of these units are gathered, respectively. These outputs are equal to several sub-performance function. Then all of the outputs are collected in order to guarantee minimize the multiple-input multiple-output (MIMO) system. Consider a MIMO system

$$\begin{aligned}
&\frac{d}{dt}\tilde{x}_1 = f_1(\tilde{x}_1, u_1), \quad \tilde{y}_1 = \tilde{F}_1(\tilde{x}_1),\\
&\frac{d}{dt}\tilde{x}_2 = f_2(\tilde{x}_2, u_2), \quad \tilde{y}_2 = \tilde{F}_2(\tilde{x}_2),\\
&\qquad\vdots\\
&\frac{d}{dt}\tilde{x}_M = f_M(\tilde{x}_M, u_M), \quad \tilde{y}_M = \tilde{F}_M(\tilde{x}_M),
\end{aligned}$$

with total performance function $J = \tilde{y}_1 + \tilde{y}_2 + \cdots + \tilde{y}_M$, where $\tilde{x}_i \in R^n$, $u_i \in R$, $\tilde{y}_i \in R$, $(i = 1, 2, \cdots, M)$ are the states, control inputs and outputs, respectively.

The aim of this section is to extend the minimization of the SISO case to the minimization of the MIMO case. There exists a minimum point J when $\tilde{y}_i = \tilde{y}_{i*}, \quad (i = 1, 2, \cdots, M)$, in which $\tilde{y}_{i*}$ is the minimal value for each sub-performance function $\tilde{y}_i$. Thus, a series of FO ESCs

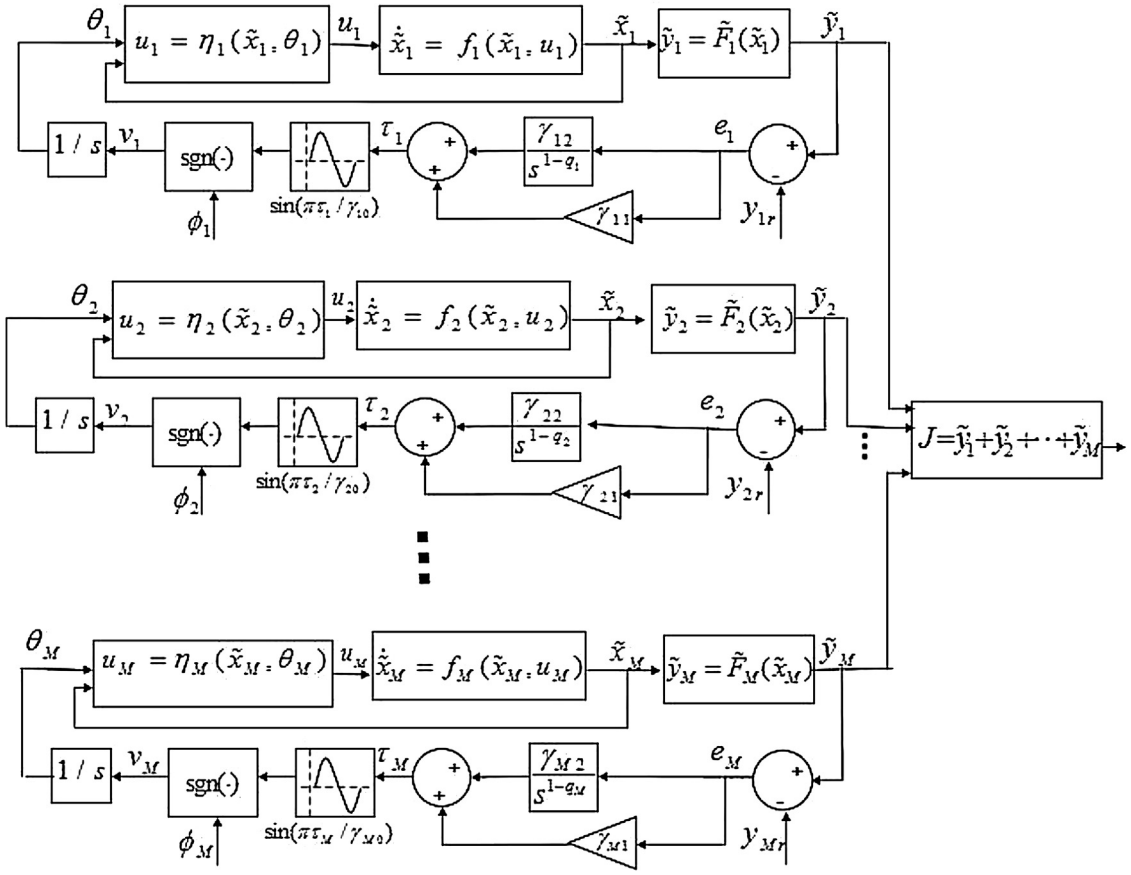

Fig. 9. Block diagram of the FO ESC in the MIMO frame.

with FO PI sliding surface are given. θ_i, $(i = 1, 2, \cdots, M)$ are proposed to satisfy $\dot{\theta}_i = v_i$, with v_i being variable structure control

$$v_i = \phi_i \mathrm{sgn}\left(\sin\left(\frac{\pi}{\gamma_{i0}}\tau_i\right)\right), \tag{7}$$

in which ϕ is a designed function,

$$\tau_i = \gamma_{i1} e_i + \gamma_2 ({}_0D_t^{q_i - 1} e_i), \quad -1 < q_i \le 0, \tag{8}$$

where $\gamma_{ij} > 0$, $(i = 1, 2, \cdots, M, j = 0, 1, 2)$, q_i are fractional order. Define $e_i = \tilde{y}_i - y_{ir}$, in which $y_{ir}(t) = -k_{ir1}t^3 - k_{ir2}t$, $y_{ir}(0) = y_{ir0}$, with $k_{ir1} \ge 0, k_{ir2} \ge 0$. The block diagram is depicted in Fig. 9. According to the investigation in Sections 3 and 4, the series of FO ESC can be separately applied to subsystem, so as to guarantee $\tilde{y}_i$ converge to $\tilde{y}_i^*$. Finally, it can minimize the total performance function J.

Remark 5.1. The light system of the two story smart house can be considered a two-input-two-output plant. Thus, when $M = 2$, one could use the above control method to realize the total minimal energy usage.

6. Experimental results

The Arduino based miniature house shown in Fig. 10 is built on Arduino hardware and Simulink. The design of the proposed minimum energy cognitive lighting control is described

$$\dot{\omega} = v, \quad E = (\omega I)^2 + ((1 - \omega)I)^2. \tag{9}$$

To minimize E, FO PI sliding surface is chosen as $\tau = \gamma_1 e + \gamma_2 ({}_0D_t^{q-1} e)$.

Case 1. In this case, all the six LEDs are chosen as white and the details are stated in Section 2. In Fig. 6, the minimal energy usage point is about at 0.2283. $E < E^* + 27\,\%$, when $0.8081 \ge \omega > 0.3635$. The

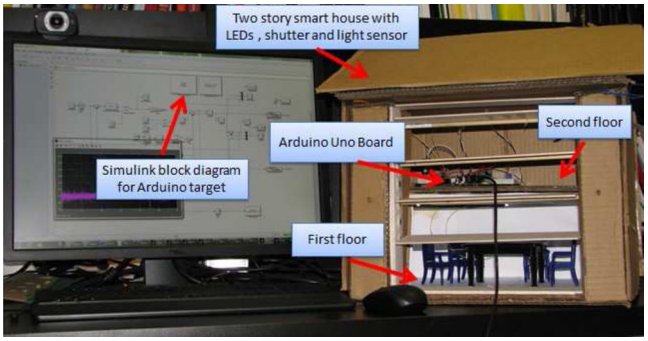

Fig. 10. The Arduino-based miniature house.

proposed FO ESC (8) is applied to minimize E. Meanwhile, the PID controller with the proportional gain $k_p = 0.9$, the integral gain $k_i = 3.5$ and the derivative gain $k_d = 0$ is employed as the tracking control for light level.

FO ESC law with $q = -0.35$ is adopted. The constant modulation function is $\phi(t) = (\gamma_1 + \gamma_2)/\varepsilon + \alpha$. The reference signal $\dot{y}_r = -0.5$, $y_r(0) = -2000$ and $\varepsilon = 0.5\gamma_0$. The design parameters are $\gamma_0 = 0.08$; $\gamma_1 = 0.000093$, $\gamma_2 = 0.005$. Response of the energy usage under FO ESC is illustrated in part (a) of Fig. 11, while the illumination under the PID controller reaches the desired light level in part (b) of Fig. 11. It is shown that E converges to E^* with an acceptable convergence speed. Meanwhile, Fig. 12 illustrates that ω tends to reach ω^* which minimizes E. The time response of τ shows the oscillations of ω.

Next, the comparison between light energy usages under $q = -0.35$ and $q = 0$ is shown in Fig. 13. It can be seen that

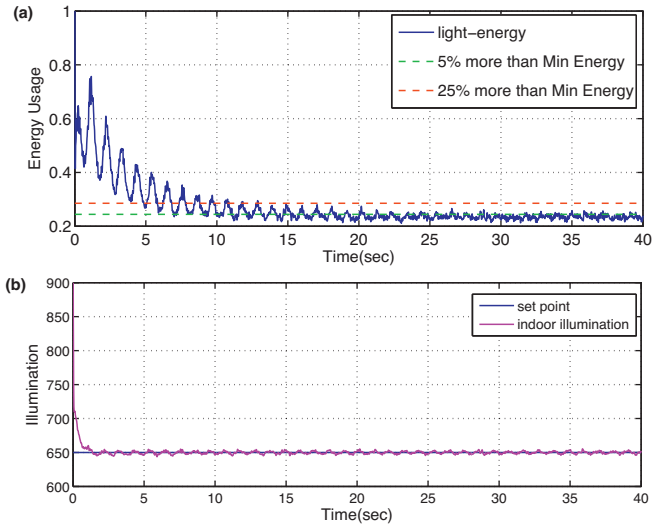

Fig. 11. (a) Time responses of the energy usage E under the FO ESC with $q = -0.35$; (b) the illumination under the PID controller of the two story smart house.

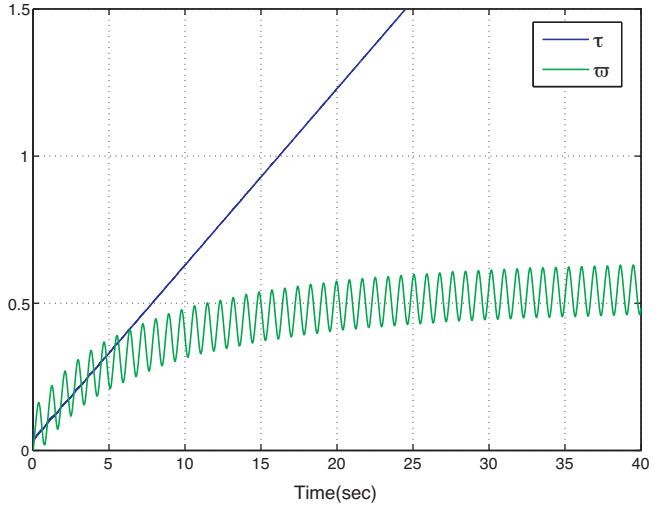

Fig. 12. Zoom in the time responses of τ showing the oscillations of ω around ω^*.

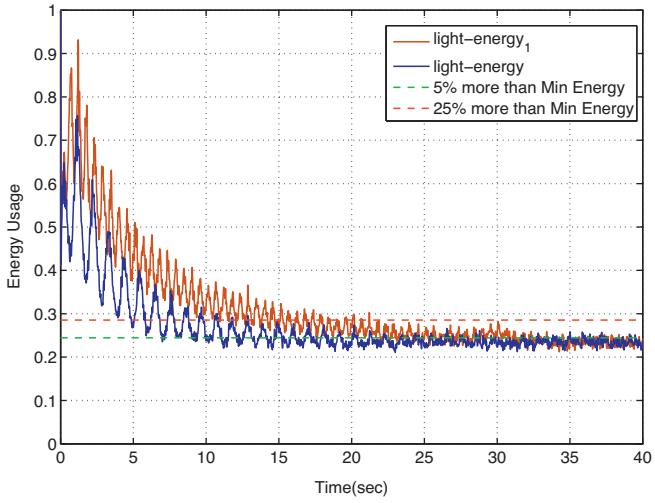

Fig. 13. Time responses of E for different integration orders in the FO ESC, in which light-energy under $q = -0.35$, light-energy1 under $q = 0$

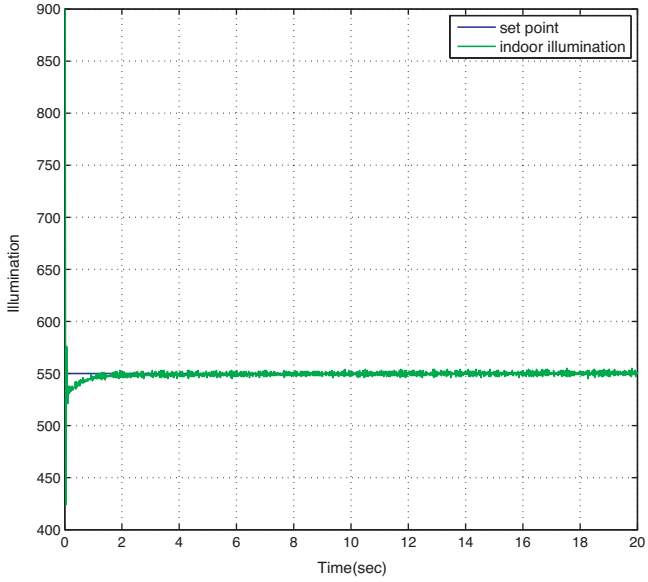

Fig. 14. The illumination of the Arduino-based smart house under PID control.

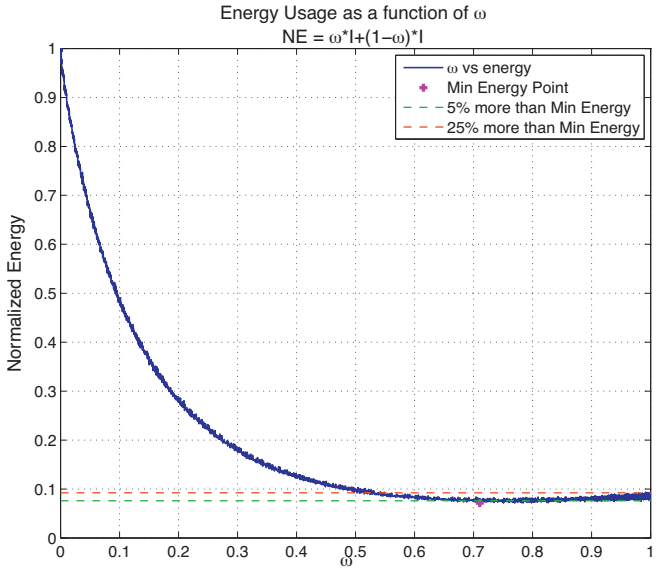

Fig. 15. E–ω curve, while the indoor illumination reaches the desired lighting level.

light-energy with $q = -0.35$ reaches E^* more rapidly when compared with light-energy1 with $q = 0$. Clearly, the flexibility make FO ESC a powerful tool in achieving to a better control performance.

Case 2. In this case, the desired light level (set point) is set to 550 out of 1023 which denotes the maximum illumination that the Arduino hardware can provide. The natural light is altered and the interior environment is changed slightly in terms of furniture positions. The indoor illumination via PID controller with $k_p = 0.8$, $k_i = 3.5$, $k_d = 0$ can reach the desired light level, as drawn in Fig. 14. At the same time, the changes in E versus ω is depicted in Fig. 15. From Figs. 14 and 15, while maintaining the set point, there exists an optimal ω^* such that $E = E^*$. It is apparent that the minimal energy usage E^* of the lighting system is about 0.07397 at $\omega = 0.7141$ in this situation. Moreover, $E < E^* + 25\,\%$, when $0.5198 \leq \omega \leq 1$.

Next, FO ESC will be applied to this case. The constant modulation function is $\phi(t) = (\gamma_1 + \gamma_2)/\varepsilon + \alpha$. The reference signal $\dot{y}_r = -0.5$, $y_r(0) = -2000$ and $\varepsilon = 0.5\gamma_0$. The design parameters are $\gamma_0 = 0.06$; $\gamma_1 = 0.00001$, $\gamma_2 = 0.04$. In order to verify the advantage of

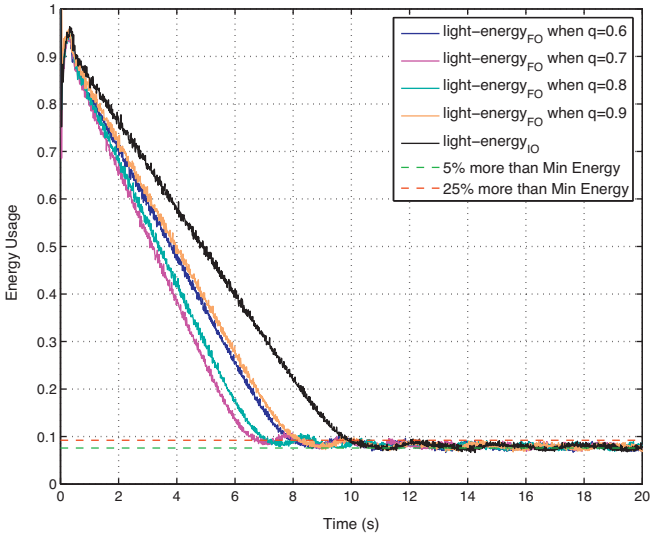

Fig. 16. Time responses of light-energy$_{FO}$ and light-energy$_{IO}$ for different integration orders (q = 0.1, 0.2, 0.3, 0.4) in the FO ESC.

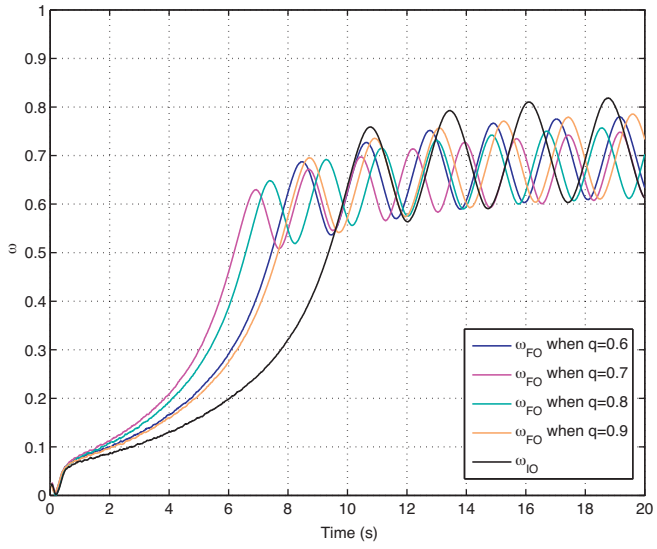

Fig. 17. Time responses of the corresponding ω_{FO} and ω_{IO}, when q = 0, 0.1, 0.2, 0.3, 0.4.

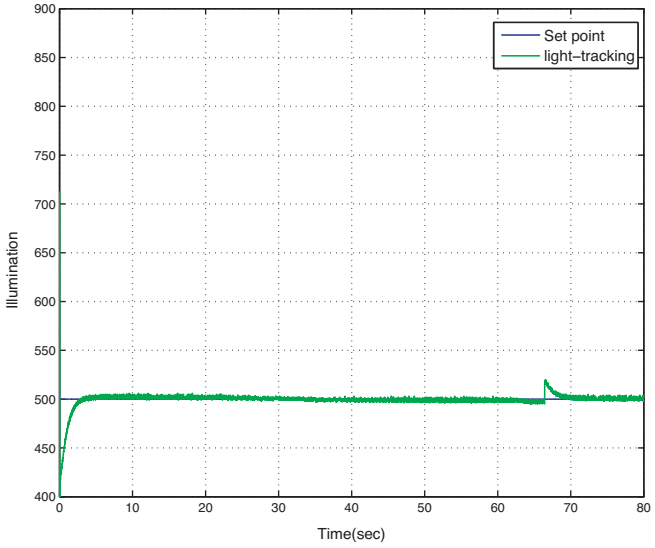

Fig. 18. The illumination of the Arduino-based smart house under PID control.

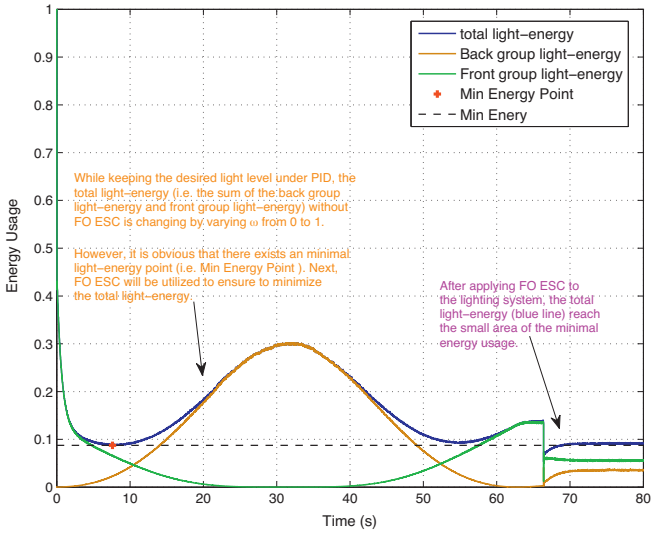

Fig. 19. Time responses of light-energy$_{FO}$ when q = 0.12.

the adaptive minimum energy lighting control, the different results are performed while q is changed. Fig. 16 shows the time responses of the energy usages under FO ESC with q = 0, 0.1, 0.2, 0.3, 0.4, respectively. It is obvious that light-energy$_{FO}$ under FO ESC with q = 0.1, 0.2, 0.3, 0.4 reach more rapidly at E^*, when compared with light-energy$_{IO}$ under IO ESC. The corresponding time responses of ω are shown in Fig. 17. It shows that ω_{FO} can reach more quickly at a smaller vicinity than ω_{IO} does. The experimental results show the effectiveness and advantage of the proposed FO minimum energy cognitive light control scheme.

Remark 6.1. The main property of ESC is tracking a varying optimum (maximum or minimum) of the performance function. This is the reason why ESC can be utilized to solve the minimal energy usage for lighting system. Figs. 18 and 19 are given to illustrate how the controller reacts in the lighting system (*the light level is set to 500 out of 1023 at the moment*). While keeping the desired light level under PID, the total light-energy usage (i.e. the sum of the back group light-energy and front group light-energy) without FO ESC is changing by varying ω from 0 to 1. It is obvious that there exists a minimal light-energy point (i.e. Min Energy Point E^* = 0.08754). Next, FO ESC with q = 0.12 and the other above parameters will be utilized to ensure to minimize the total light-energy. At t = 66 s, FO ESC is applied to the lighting system. It can be found that the total light-energy can approach to a small vicinity of E^*, while maintaining the desired light level.

Remark 6.2. One important requirement is huge electrical energy saving, which is possible by developing suitable energy efficient devices, effective controls and careful design. In Refs. [5–11], linear programming method has been applied to accomplish to minimize the illuminance. This paper considers how to further reduce electricity energy consumption for the desired illumination levels by manipulating different light sources. In order to easily show and explain the effectiveness of the proposed control strategy, a constant natural light is assumed and a set point light level is chosen. The experimental results demonstrate the practicality and effectiveness of the proposed lighting control scheme. Next, we will discuss how to further reduce energy consumption under more complex situations in our further work. In detail, the proposed control strategy may be improved to further minimize electrical

energy usage of the lights, while the linear programming method can achieve to the minimum illuminance.

7. Conclusions

In this paper, the FO minimal energy cognitive lighting control was proposed to cut electric energy usage in the hybrid lighting system. The Arduino-based miniature two-story smart house was built. The FO ESC with the FO PI sliding surface can improve convergence speed to the electric minimal energy usage, while the indoor illumination under the PID controller can reach the desired light level. Experimental results were used to show the effectiveness and applicability of the proposed design method.

Future works will focus on how to further reduce electrical energy consumption in a more complex situation. Combine linear programming method with the FO ESC may be investigated to accomplish to further save electrical energy usage in a more complex situation. Moreover, how to combine linear programming method with the FO ESC will also be discussed to further save electrical energy usage of the MIMO system in more complex situation.

Appendix A. Relation between ADC value with illumination

The Arduino has a 10bit Analog to Digital Converter (ADC). To convert the ADC values to voltage, we use $V = 5 \times (ADC/1024)$. The photocell uses a voltage divider to generate a voltage to measure. The resistor used in the physical test plant is a 10 kΩ. On the other hand, the equation to calculate voltage from a resistor divider is $V = 5 \times ((R_2)/(R_1 + R_2))$, where $R_1 = 10\text{k}\Omega$ resistor and R_2 is the resistance of the photocell. From the datasheet, we have the following equation $lux = 300 \times {R_2}^{-1.9}$ where R_2 is the resistance of the photocell. Thus, it can be obtained $5 \times (ADC/1024) = 5 \times ((R_2)/(R_1 + R_2))$. Furthermore, one can conclude that $R_2 = (ADC \times R_1)/(1024 - ADC)$. Thus, one has $lux = 300 \times ((ADC \times R_1)/(1024 - ADC))^{-1.9}$. In our figures, we use the ADC dates that the Arduino hardware provides to represent illumination. They can converter to lux.

Appendix B. Proof of Theorem 4.1

Consider the non-negative functions [16], $W_1(\tau) = \int_0^\tau \text{sgn}\left(\sin\left(\pi\epsilon/\gamma_0\right)\right) d\epsilon$, $W_2(\tau) = \gamma_0 - W_1$. The time derivative of W_1 and W_2 are obtained

$$\dot{W}_1 = k\left\{\phi \text{sgn}^2\left(\sin\left(\frac{\pi}{\gamma_0}\tau\right)\right) + \varpi \text{sgn}\left(\sin\left(\frac{\pi}{\gamma_0}\tau\right)\right)\right\} + \gamma_1 k_{r1} t^2 \text{sgn}\left(\sin\left(\frac{\pi}{\gamma_0}\tau\right)\right)$$

$$\dot{W}_2 = -\dot{W}_1.$$

Hence, from $|k||\varpi| \le |k|\hat{\varpi}$, one can derive $\dot{W}_1 \le -|k|\{\phi - \hat{\varpi}\} + \gamma_1 k_{r1} t^2$, if $\text{sgn}(k) < 0$, $\dot{W}_2 \le -|k|\{\phi - \hat{\varpi}\} + \gamma_1 k_{r1} t^2$, if $\text{sgn}(k) > 0$. On the other hand, one has $-|k| \le \tilde{k}$. Thus, it has that $\dot{W}_1 \le -||y_t||e^{-\alpha_1 t} - \tilde{k}\alpha + \gamma_1 k_{r1} t^2$, if $\text{sgn}(k) < 0$, or $\dot{W}_2 \le -||y_t||e^{-\alpha_1 t} - \tilde{k}\alpha + \gamma_1 k_{r1} t^2$, if $\text{sgn}(k) > 0$, hold almost everywhere with $\alpha \ge 0, \alpha_1 > 0$.

Property (i): Assume that $|\tau(t)|$ evades in the finite time $t_1 \in [0, t_M)$. Then, from (8), $e(t)$ and $y(t)$ also can evades at $t = t_1$. Hence, there exists $t_2 \in [0, t_1)$ such that $||y_t|| \ge e^{\alpha_1 t}[\alpha_2 - \tilde{k}\alpha + \gamma_1 k_{r1} t_1^2]$, in which $\alpha_2 \ge 0$. Moreover, one has

$$\begin{aligned} &\dot{W}_1 \le -\alpha_2 - \gamma_1 k_{r1} t_1^2 + \gamma_1 k_{r1} t^2 \le -\alpha_2, \quad \forall t \in [t_2, t_1), \\ \text{or} \quad &\dot{W}_2 \le -\alpha_2 - \gamma_1 k_{r1} t_1^2 + \gamma_1 k_{r1} t^2 \le -\alpha_2, \quad \forall t \in [t_2, t_1), \end{aligned} \tag{B.2}$$

independently of $\text{sgn}(k)$. Since $\tau(t)$ is absolute continuous and evades in $t = t_1$, there exists $t_e \in [t_2, t_1)$ and $l_\tau \in N$ such that $\tau(t_e) = l_\tau \gamma_0$. Therefore, $W_1(t_e) = 0$ (for even number l_τ) or $W_2(t_e) = 0$ (for odd number l_τ). Obviously, $W_1(t) = 0$ or $W_2(t) = 0$, $\forall t \in [t_e, t_1)$ in this interval. $W_i(\tau(t))$ can be changed by $W_i(t)$, for $i = 1, 2$. Hence, $\tau(t) = l_\tau \gamma_0$ is uniformly bounded $\forall t \in [t_e, t_1)$, i.e., a contradiction. Thus, τ, e, y cannot evade in finite time.

Property (ii): there exists $\bar{t} \ge 0$ such that $\dot{W}_i \le -\alpha_{\bar{t}}$, $\forall t \ge \bar{t}$ and $0 < \alpha_{\bar{t}} < \tilde{k}\alpha$, for $i = 1$ or 2. Thus, $W_i(t) \le -\alpha_{\bar{t}}(t - \bar{t}) + W_i(\bar{t})$, $\forall t \ge \bar{t}$. There exists $t* \ge \bar{t}$ such that $W_i(t) = 0, \forall t \ge t^*$. Moreover, $\tau = l\gamma_0$ for which $W_1(\tau) = 0 (W_2(\tau) = 0)$ happens at only for even(odd) value of l. In the small vicinity around $\tau = l\gamma_0$, $\text{sgn}\left(\sin\left(\pi\tau/\gamma_0\right)\right) = \text{sgn}(\tau - l\gamma_0)$ for even number l, or $\text{sgn}(\sin(\pi\tau/\gamma_0)) = -\text{sgn}(\tau - l\gamma_0)$, for odd number l. Selecting $V = 0.5(\tau - l\gamma_0)^2$, one has

$$\dot{V} = (\tau - l\gamma_0)(k(\phi \text{sgn}(\sin(\pi\tau/\gamma_0)) + \vartheta)) \le -\alpha|\tau - l\gamma_0| \le 0, \quad \forall t \ge t*. \tag{B.3}$$

Hence, a sliding mode happens in finite time on one of the FO PI sliding manifolds $\tau = l\gamma_0$, independently of $\text{sgn}(k)$.

Appendix C. Proof of Theorem 4.2

The proof of Theorem 4.2 will be given as follows: (i)Attractiveness of D_δ: Assume that $\theta \notin D_\delta$, $\forall t \in [0, t_M)$. From Theorem 4.1, there exists a finite time t_f such that $\dot{\tau} = 0$. Hence, ${}_0D_t^{1-q} e = -(\gamma_2/\gamma_1)e, \forall t \ge t_f$. Since $-1 < q < 0$, one has $|\arg(eig(-\gamma_2/\gamma_1))| > (1 - q)\pi/2$. So the dynamics ${}_0D_t^{1-q} e = -(\gamma_2/\gamma_1)e, (\forall t \ge t_f, -1 < q < 0)$ is asymptotically stable from Lemma 3.1. Thus, y_r draws y close in y^*. On the other hand, $y \ge y^*$ and y_r strictly decreases with time. Thus, for $-1 < q < 0$, one has $y_r < y^* \le y$, $e > 0$ and ${}_0D_t^q e > 0$ when t is large enough. So y decreases with the negative rate $(\dot{y} = -k_{r1}t^2 - k_{r2} - (\gamma_2/\gamma_1)({}_0D_t^q e) < 0)$ when t is large enough, that is, $y = F(\theta)$ must continue to approach y^*. Hence, θ goes to D_δ, which is a contradiction. Thus, D_δ is attained in some finite time. So, θ remains or oscillates around D_δ. y stays or oscillates in some small vicinity of y^*. Next, we will show that $|y - y^*|$ can be made ultimately of order $O(\gamma_0)$.

(ii) Oscillations of order $O(\gamma_0)$ around y^*: From Assumption 3.3, δ can be made arbitrarily small such that $|y - y^*| = O(\gamma_0)$ when $\theta \in D_\delta$. Thus, if θ stays in $D_\delta, \forall t$, the oscillations around y^* can be made of order $O(\gamma_0)$. Otherwise, it is important to show that $|y - y^*| = O(\gamma_0)$ holds if θ oscillates around D_δ.

Obviously, there exists C such that $\bar{B} \le y_r < y* \le y < C, \forall t$ large enough. Thus, there exists $\tilde{t} > 0$ such that $e(t) > 0, \forall t > \tilde{t}$. Note that D_δ is invariant when $\tau(t)$ is in the FO switching surface. Define $\tilde{\tau}(t) = \tau(t) - \tau(\tilde{t}_1), \tilde{y}(t) = y(t) - y(\tilde{t}_1)$, one has

$$\dot{\tilde{\tau}}(t) = \gamma_1 \tilde{y}(t) + \gamma_1 k_{s1}(t^3 - \tilde{t}_1^3) + \gamma_1 k_{s2}(t - \tilde{t}_1) + \gamma_2({}_{\tilde{t}_1}D_t^{q-1} e), \quad -1 < q < 0. \tag{C.1}$$

in which $k_{s1} = 0$, $k_{s2} = 0$ if y_r is saturated and $k_{s1} = k_{r1}$, $k_{s2} = k_{r2}$, otherwise. From Lemma 3.2, there exists K such that $|{}_0D_t^{q-1} e| < K|e|$. Thus, for $t > \tilde{t}_1 > \tilde{t}$, one has $|y(t) - y_r(t)| \le C - \bar{B}$. So $|\tilde{y}(t)| \le \gamma_1|\tilde{\tau}(t)| + \gamma_1 k_{s1}(t^3 - \tilde{t}_1^3) + (\gamma_1 k_{s2} + \gamma_2 K(C - \bar{B}))(t - \tilde{t}_1)$. Let $\tilde{t}_2$ be the first time when $\tau(t)$ reaches the next sliding manifold $\tau(t) = \tau(\tilde{t}_2)$ (independently if θ is inside or outside D_δ) and $\tilde{t}_3$ is the first time when θ reaches the frontier of D_δ again (from outside). One has $\tilde{t}_2 \ge \tilde{t}_1, \tilde{t}_3 \ge \tilde{t}_1$. There are two cases: (I) $\tilde{t}_3 \le \tilde{t}_2$ and (II) $\tilde{t}_3 > \tilde{t}_2$.

For case (I), let $t \in [\tilde{t}_1, \tilde{t}_2]$. $\tau(t)$ is not in sliding motion during $[\tilde{t}_1, \tilde{t}_2)$. Hence, there exists an integer l such that $l\gamma_0 < \tau(t) < (l + 1)\gamma_0$ and $\text{sgn}(\sin(\pi\tau(t)/\gamma_0)) \ne 0$. Otherwise, sliding mode happens at $\tau(t) = l\gamma_0$ or $\tau(t) = (l + 1)\gamma_0$. Hence, $\tilde{\tau}(t)$ is of order $O(\gamma_0)$, $\forall t \in [\tilde{t}_1, \tilde{t}_2)$. Moreover, $|\text{sgn}(\sin(\pi\tau(t)/\gamma_0))| = 1, \forall t \in [\tilde{t}_1, \tilde{t}_2)$. One has $|\dot{\tilde{\tau}}(t)| \ge \tilde{k}(|\phi| - |\varpi|) - \gamma_1 k_{r1} \tilde{t}_2^2 \ge \tilde{\alpha}$ in which $\tilde{\alpha} = \tilde{k}\alpha - \gamma_1 k_{r1} \tilde{t}_2^2$. Here, one can require that $\alpha > 0$ satisfies $\tilde{k}\alpha > \gamma_1 k_{r1} \tilde{t}_2^2$. Thus, $(t - \tilde{t}_1) \le$

$|\tilde{\tau}|/\tilde{\alpha}$, $\forall t \in [\tilde{t}_1, \tilde{t}_2)$ and $(t - \tilde{t}_1)$ is of order $O(\gamma_0)$, $\forall t \in [\tilde{t}_1, \tilde{t}_2)$. Since $t^3 - \tilde{t}_1^3 = (t - t_1)(t^2 + \tilde{t}_1^2 + t\tilde{t}_1)$. Since $t \in [\tilde{t}_1, \tilde{t}_2)$, one has $(t^2 + \tilde{t}_1^2 + t\tilde{t}_1) < \zeta$ in which $\zeta = \tilde{t}_2^2 + \tilde{t}_1^2 + \tilde{t}_2\tilde{t}_1$. Therefore, $t^3 - \tilde{t}_1^3 \leq |\tilde{\tau}|\zeta/\tilde{\alpha}$, $\forall t \in [\tilde{t}_1, \tilde{t}_2)$. Thus, $(t^3 - \tilde{t}_1^3)$ is of order $O(\gamma_0)$, $\forall t \in [\tilde{t}_1, \tilde{t}_2)$. Hence, $y(t) - y(\tilde{t}_1)$ is of order $O(\gamma_0)$, $\forall t \in [\tilde{t}_1, \tilde{t}_2)$. By continuity, $y(t) - y(\tilde{t}_1)$ is also of order $O(\gamma_0)$, $\forall t \in [\tilde{t}_1, \tilde{t}_2]$.

For case (II), let $t \in [\tilde{t}_1, \tilde{t}_3]$. From case (I), $y(t) - y(\tilde{t}_1)$ is of order $O(\gamma_0)$, $\forall t \in [\tilde{t}_1, \tilde{t}_2]$. Next, consider $t \in [\tilde{t}_2, \tilde{t}_3]$. Since $\tau(t)$ is in sliding motion during $[\tilde{t}_2, \tilde{t}_3]$, one has $\dot{\tau}(t) = 0$. Thus, $y(t)$, $\forall t \in [\tilde{t}_2, \tilde{t}_3]$ is decreasing with $\dot{y} = -k_{s1}t^2 - k_{s2} - (\gamma_2/\gamma_1)_0 D_t^q e < 0$. Hence, $y(t)$ continues to close in y^* during $[\tilde{t}_2, \tilde{t}_3]$. $y(t) - y(\tilde{t}_1)$ is also of order $O(\gamma_0)$, $\forall t \in [\tilde{t}_2, \tilde{t}_3]$. Combining (I), $y(t) - y(\tilde{t}_1)$ is of order $O(\gamma_0)$, $\forall t \in [\tilde{t}_1, \tilde{t}_3]$.

References

[1] P. Kozodoy, S.P. DenBaars, A.J. Heeger, White light from InGaN/conjugated polymer hybrid light-emitting diodes, Appl. Phys. Lett. 70 (1997) 2664–2666.
[2] A. Guillemin, N. Morel, An innovative lighting controller integrated in a self-adaptive building control system, Energy Build. 33 (2001) 477–487.
[3] C. Reinhart, A. Fitz, Findings from a survey on the current use of daylight simulations in building design, Energy Build. 38 (2006) 824–835.
[4] A. Rosemann, M. Mossman, L. Whitehead, Development of a cost-effective solar illumination system to bring natural light into the building core, Solar Energy 82 (2008) 302–310.
[5] M. Miki, A. Amamiya, T. Hiroyasu, Distributed optimal control of lighting based on stochastic hill climbing method with variable neighborhood., in: IEEE International Conference on Systems, Man and Cybernetics, 2007, pp. 1676–1680.
[6] B. Roisin, M. Bodart, A. Deneyer, P.D. Herdt, Lighting energy savings in offices using different control systems and their real consumption, Energy Build. 40 (2008) 514–523.
[7] Y.-W. Bai, Y.-T. Ku, Automatic room light intensity detection and control using a microprocessor and light sensors, IEEE Trans. Consum. Electr. 54 (2008) 1173–1176.
[8] D. Caicedo, A. Pandharipande, Daylight integrated illumination control of LED systems based on enhanced presence sensing, Energy Build. 43 (2011) 944–950.
[9] Y.-J. Wen, A.M. Agogino, Personalized dynamic design of networked lighting for energy-efficiency in open-plan offices, Energy Build. 43 (2011) 1919–1924.
[10] D. Caicedo, A. Pandharipande, Distributed illumination control with local sensing and actuation in networked lighting systems, IEEE Sens. J. 13 (2013) 1092–1104.
[11] D. Caicedo, A. Pandharipande, F.M.J. Willems, Daylight-adaptive lighting control using light sensor calibration prior-information, Energy Build. 73 (2014) 105–114.
[12] C. Yin, B. Stark, S.M. Zhong, Y.Q. Chen, Minimum Energy Cognitive Lighting Control: Stability Analysis and Experiments, in: ASME IDETC/CIE 2013, Portland, OR, 2013, pp. 1–8.
[13] C. Yin, B. Stark, Y.Q. Chen, S.M. Zhong, Adaptive minimum energy cognitive lighting control: Integer order vs fractional order strategies in sliding mode based extremum seeking, Mechatronics 23 (2013) 863–872.
[14] M. Krstić, H.H. Wang, Stability analysis of extremum seeking feedback for general nonlinear systems, Automatica 36 (2000) 595–601.
[15] Y. Pan, Ü. Özgüner, Stability and performance improvement of extremum seeking control with sliding mode, Int. J. Control 76 (2003) 968–985.
[16] T.R. Oliveira, A.J. Peixoto, E.V.L. Nunes, L. Hsu, Global real-time optimization by output-feedback extremum-seeking control with sliding modes, J. Frankl. Inst. 349 (2012) 1397–1415.
[17] Arduino. http://www.arduino.cc
[18] http://www.sparkfun.com/products/11227, Sparkfun Inventor's Kit.
[19] I. Podlubny, Fractional Differential Equations, Academic Press, 1999.
[20] S.G. Samko, A.A. Kilbas, O.I. Marichev, Fractional Integrals and Derivatives: Theory and Applications, Gordon and Breach Science Publishers, Switzerland, 1993.
[21] D. Matignon, Stability properties for generalized fractional differential systems, ESAIM: Proc 5 (1998) 145–158.
[22] C. Yin, S.M. Zhong, W.F. Chen, Design of sliding mode controller for a class of fractional-order chaotic systems, Commun. Nonlinear Sci. Numer. Simulat. 17 (2012) 356–366.
[23] Y. Luo, Y.Q. Chen, Fractional order [proportional derivative] controller for a class of fractional order systems, Automatica 45 (2009) 2446–2450.
[24] C. Yin, Y.Q. Chen, S.M. Zhong, Fractional-order sliding mode based extremum seeking control of a class of nonlinear systems, Automatica (2014), http://dx.doi.org/10.1016/j.automatica.2014.10.027.